

Article

Influence of Urban Geometry on Thermal Environment of Urban Street Canyons in Hong Kong

Shanshan Zhu ¹, Mingyue Chen ², Shiyao Lu ³ and Xianmin Mai ^{4,*}

¹ Faculty of Architecture, Southwest Jiaotong University, Building and Design Hall, Building 8, West High-Tech Zone, Chengdu 611756, China

² Faculty of Architecture, The University of Hong Kong, Queen's Road West 537, Hong Kong

³ BEE Incorporations, Suite 1103A-04, Nanyang 1931 Plaza, 165 Yude Road, Xuhui District, Shanghai 200030, China

⁴ School of Architecture, Southwest Minzu University, 16 South Fourth Section, First Ring Road, Chengdu 610041, China

* Correspondence: maixianmin@foxmail.com

Abstract: Hong Kong is a typical high-density city in a subtropical climate region, and deep street canyons are among the main features of its urban planning. How the urban geometry influences the urban thermal environment in this city has become a hot topic these days. The height-to-width ratio (H/W) and sky view factor (SVF) are commonly used to indicate the outdoor thermal environment performance, while previous studies in Hong Kong rarely analysed the importance bias of these two influencing factors systematically in this context. To fill this research gap, in this paper, we chose four typical sites in Hong Kong as research objects. Firstly, we conducted a field investigation to calculate the main influencing factors of urban street geometry (H/W and SVF) and then used field measurements to collect climatic data, including air temperature, wind speed, and relative humidity, and finally used regression to analyse the correlation between H/W, SVF, and temperature. The results indicate the following: (1) There is a greater correlation between H/W and air temperature than between SVF and air temperature by regression analysis, and H/W is more effective at improving the thermal environment within urban street canyons. (2) After field measurements, it was found that H/W at the measurement sites was 0.60 to 6.02, with an average of 2.13. (3) In the study area, H/W of 2.31–2.48 and 3.35–3.60 had a positive correlation with air temperature, and H/W had a dominant influence on outdoor air temperature, and H/W of 2.09–2.31 and H/W > 3.60 was inversely related to air temperature. The conclusions can provide support for urban planning in Hong Kong.

Keywords: thermal environment; urban street canyon; urban geometry; height-to-width ratio (H/W); sky view factor (SVF)



Citation: Zhu, S.; Chen, M.; Lu, S.; Mai, X. Influence of Urban Geometry on Thermal Environment of Urban Street Canyons in Hong Kong. *Buildings* **2022**, *12*, 1836. <https://doi.org/10.3390/buildings12111836>

Academic Editors: Bo Hong, Dayi Lai, Zhi Gao, Yongxin Xie and Kuixing Liu

Received: 28 September 2022

Accepted: 27 October 2022

Published: 1 November 2022

Publisher's Note: MDPI stays neutral with regard to jurisdictional claims in published maps and institutional affiliations.



Copyright: © 2022 by the authors. Licensee MDPI, Basel, Switzerland. This article is an open access article distributed under the terms and conditions of the Creative Commons Attribution (CC BY) license (<https://creativecommons.org/licenses/by/4.0/>).

1. Introduction

1.1. Basic Information of Hong Kong

Hong Kong is a coastal city in southern China, connected to Shenzhen to the north and the south China Sea (22°17' N, 114°09' E), and has a humid subtropical climate. Summer is the hottest and most humid season, while winter is more comfortable. The summer season usually lasts seven months, from May to November [1]. Therefore, heat and humidity in the summer is the main weather problem in Hong Kong compared to winter weather, as it is more likely to cause heat stress in urban areas. In addition, Hong Kong is also one of the most densely populated cities in the world, with a population density of 7132.25 people per square kilometre [2], and it has become extremely common to have residential spaces on narrow streets of 15–25 metres between approximately 40-to-60-storey buildings (Figure 1) [3]. These conditions have led to the formation of unique street canyons, making it more difficult for air above the street canyon level to pass through deeper canyons. The urban heat environment is currently a hot research topic in Hong Kong, triggered not only by global warming and the urban heat island (UHI) effects but

also by epidemics, as the city has been severely hit by COVID-19 since 2020 in response to which the government introduced a mask law requiring people to wear masks when going out on the streets to reduce the number of infections and protect public health (Figure 2). This has undoubtedly also led to a higher demand by the public for a warmer environment on the streets. Therefore, how urban street canyons affect local microclimates and human thermal comfort during the daytime in summer has become a major planning issue in Hong Kong.



Figure 1. High-density high-rise buildings in Hong Kong [4].



Figure 2. People walking in Central District of Hong Kong wearing masks for protection against COVID-19 [5].

1.2. Current Study Situation

Globally, many scholars have studied the thermal environment of urban canyons, comparing it with other parameters such as solar path, building coverage, greenery coverage, and paving materials [6–8]. Studies show that the influential urban geometry factors H/W and SVF have a significant impact on the thermal environment, while in Hong Kong, the latest results indicate that current studies are more focused on quantifying and analysing the SVF effect on the thermal environment. Meanwhile, some scholars have conducted research on the urban thermal environment using Google Street View (GSV) images [9], but rarely have they mentioned the effect of H/W on outdoor thermal environment performance. Thus, it is necessary to find the correlation between H/W, SVF, and the thermal environment in order to clearly determine the dependence of the thermal environment of urban street canyons on urban geometry for future urban planning.

1.3. Research Objectives

In order to fill this research gap, we use urban geometry to study the outdoor thermal environment in Hong Kong at the street level and selected H/W and SVF as the study parameters to quantify their impact on the thermal environment and compare them. It is possible to determine which parameter has a greater impact on the thermal environment and, according to the regression result, find correlations between the influencing factors on the urban thermal environment to provide guidance for future urban planning in Hong Kong.

2. Literature Review

2.1. Effect of Urban Street Canyon Design on Thermal Environment

According to current research, many design aspects of urban street canyons, such as H/W and SVF, are noted to have a significant impact on the thermal environment of urban streets [10]. Even though other design factors, such as building coverage, greenery coverage, building and paving materials, and land use, also partly influence outdoor thermal comfort, H/W and SVF are considered to be the main influences on the thermal environment in urban street canyons. A specific analysis of the relationship between H/W and SVF and the urban thermal environment is available in the relevant literature.

2.1.1. H/W

H/W is the ratio between the height of a building (H) and the width of the street between buildings (W) in two-dimensional (2D) form and has a great effect on the amount of incident and outgoing solar radiation and wind distribution within urban street canyons [10–12].

Many scholars have conducted studies related to H/W in the tropics. For example, in 2005, Erik Johansson studied the influence of the geometry of the Moroccan city of Fez ($33^{\circ}158' N$, $4^{\circ}159' W$) on the outdoor thermal environment by comparing the effect of H/W on the microclimate at street level. The results of the study showed that the maximum diurnal temperature difference between the deepest street canyon ($H/W \approx 10$) and the shallowest street canyon ($H/W = 0.6$) was, on average, 6 K in summer and could reach 10 K on the hottest days. The average summer temperatures of deep and shallow street canyons compared to rural sites indicate that the cooling island effect of deep canyons is quite pronounced during hot summer days. Nighttime temperatures are higher in deep canyons than in shallow canyons because there is less open sky in deep canyons. The study also showed that in winter, shaded canyons are more comfortable than deep canyons because there is more solar access during the day [12].

A study was also conducted in the tropical city of Singapore. In this work, the researchers assessed the impact of urban geometry on outdoor thermal comfort (OTC), focusing on a new mixed-use high-rise development in the city. The authors analysed different urban design strategies/scenarios: two block forms, four street orientations (north–south, east–west, north–east–west, north–west–east), four H/W values (from 1.5 to 3.5), and three building height scenarios (height-based building alignment). The study was

based on modelling techniques. Their results showed the best OTC levels on H/W of 2.5–3 and a north–south orientation [13].

Another study simulated 36 scenarios in winter and summer for the municipality of Campinas in São Paulo, Brazil, located in the mid-latitude tropics. The simulations included space between buildings, which varied in H/W (avenue, normal, and deep canyons with $H/W = 0.5$, $H/W = 1.0$, and $H/W > 2.0$) and L/H (short, medium, and long canyons with $L/H = 3.0$, $L/H = 5.0$, and $L/H > 7.0$). The results show that canyons with higher H/W values had increased wind speed and shading from buildings, thus affecting pedestrian thermal comfort, especially in summer. In contrast, in winter, increased H/W had no significant effect on thermal comfort at the pedestrian level [14].

Muniz-Gaal et al. showed that, in Campinas, the maximum temperature was $1.0\text{ }^{\circ}\text{C}$ lower in the scenario with a higher correlation between canyon height and width ($H/W > 1.0$) than in the more open scenario ($H/W = 0.4$). The increase in H/W led to increased canyon shading and reduced daily comfort variability and peak physiological equivalent temperature (PET) [15].

Studies by Sun et al. in cold regions of China showed that shallow and weak canyons ($0.5 < H/W < 1.5$) were more favourable in cold climates, with the best streets being near the N–S direction, followed by intermediate directions, while deeper canyons ($H/W > 1.5$) were not recommended due to the lack of absorption of sunlight [16].

2.1.2. SVF

The SVF concept was first introduced by Oke in 1981 to assess the urban heat island effect [17]. More recently, it has been used as a geometric concept to provide a scale of the visible area of the sky within a street canyon, illustrated by dimensionless values [18]. Previous studies showed that the urban morphology is significantly related to local solar irradiance and air temperature [3], and in describing urban climate and its spatial variability, the skyscape factor (SVF) plays a key role.

SVF was used as the main indicator to assess the impact of urban geometry on air temperature using ENVI-met software for field measurements in the city centre of Curitiba, Brazil, which is in a tropical region. Two dependent variables were assessed in this study: diurnal heat island, defined by the temperature difference between the measurement site and the reference climate station, and $\Delta\text{MRT-T}$, calculated from the difference between the measured hourly mean radiation temperature and the ambient air temperature. It shows the correlation between SVF and $\Delta\text{MRT-T}$, which is higher than the correlation between SVF and diurnal heat island, with a coefficient of determination (R^2) of 0.35, which is higher than 0.10, indicating that the mean radiation temperature is more closely related to SVF than to ambient air temperature [18].

He et al. studied the effects of SVF on outdoor thermal conditions and PET in the Beijing Central Business District (located in Chaoyang District), which has a temperate climate with highly shaded areas in hot summers and long, cold, windy, dry winters. The findings indicated that $\text{SVF} < 0.3$ was typically associated with fewer heat conditions in summer and longer periods of cold discomfort in winter than moderately shaded areas ($0.3 < \text{SVF} < 0.5$) and lightly shaded areas ($\text{SVF} > 0.5$), and vice versa [19].

Although researchers have demonstrated the importance of SVF to the urban thermal environment, there was one exception, a study that was conducted in Kano ($12^{\circ}00' \text{ N}$, $8^{\circ}31' \text{ E}$), the largest city in northern Nigeria, a tropical region. The city has an average annual temperature of $30.75\text{ }^{\circ}\text{C}$, usually receives about 49.8 mm of precipitation, and has 62.99 rainy days per year. The average maximum temperature throughout the year is $36.33\text{ }^{\circ}\text{C}$, and the minimum temperature reaches $22.52\text{ }^{\circ}\text{C}$. The researchers found there was little relationship between SVF and temperature distribution. This result implies a generally weak influence of SVF on the temperature in that city. This suggests that other factors, such as wind, cloud cover, proximity to bodies of water, and heat release from human activity, may have a greater influence on the temperature distribution in the region [20].

In addition, SVF has been used as a research parameter when studying the relationship between subtropical high-density urban geometry and urban microclimate. A UHI study

was conducted in Hong Kong during the summer months. The results showed that SVF was highly correlated with diurnal UHI, with R^2 values of 0.7 and 0.8. The relationship between SVF and intra-urban air temperature differences within the street canyons of Hong Kong during the summer was determined by generating SVF maps of the entire urban environment using ArcGIS-based software. The study noted that SVF analysis is valid for urban microclimate studies in Hong Kong. The study also noted that regional SVF averages are more suitable for quantifying the relationship between urban geometry and intra-urban daytime temperature differences than point SVF values [3]. Regarding SVF measurement, an empirical case study was conducted based on a simulated three-dimensional (3D) urban model of a typical street canyon in Hong Kong. It shows a general trend in the negative effect of SVF on temperature difference, which suggests that smaller SVF values generally lead to higher temperature differences, however, the coefficient of determination is relatively low ($R^2 = 0.18$) [3].

2.1.3. Correlation between H/W, SVF, and Urban Thermal Environment

Past scholarly research has found that in tropical, subtropical, and Mediterranean climates, temperature cooling in summer is more effective as H/W and SVF increase [21–23]. This shows that H/W and SVF have an effect on the urban thermal environment at the same time, and which factor is greater for the urban thermal environment was analysed in the literature.

In the tropical climate of Constantine, Algeria, researchers assessed the effect of SVF on microclimate within a street canyon. In this study, the researchers set up seven sites to collect climate data and calculated SVF values and H/W for these sites. The air temperature at these sites directly indicated that lower SVF and higher H/W values led to colder conditions. The results of the study showed that the relationship between air temperature and SVF was lower than expected, with a lower coefficient of determination (R^2) based on an entire 24-h period. A higher coefficient of determination between SVF and air temperature was found between 12:00 and 18:00 ($R^2 = 0.46$) [21].

Deevi and Chundeli conducted a study in 2020 using regression of SVF and H/W, and they investigated the factors influencing the outdoor thermal comfort of a street canyon. User-perception surveys and empirical measurements using TESTO 480 and TESTO 870 thermal imagers were carried out at six selected grid points along the 600 m long, 12 m wide Besant Road, a semi-motorised commercial street in Vijayawada, Andhra Pradesh, India. SVF was the predominant physical parameter influencing thermal comfort in existing streets, while H/W slightly influenced the overall comfort condition. It was noted that SVF can be modified more easily than H/W [22].

Another study evaluated the thermal comfort of different spaces in five types of street microclimates in urban and rural Chongqing. The results showed that SVF had a more significant impact on the thermal environment of the streets than H/W. Among the various types of streets, B-N with one open side (SVF = 0.474) had the worst thermal environment, with an average universal thermal climate index (UTCI) of 44.7 °C. The two-sided closed B₂-B₂ (SVF = 0.052) had a better thermal environment, with an average UTCI of 35.5 °C. The R^2 value of 0.88 reflected a greater linear correlation between UTCI and SVF than H/W, with an R^2 value of only 0.04 [23].

2.2. Review Conclusion

According to the above findings, the conclusions of the review are summarised as follows:

- ① In terms of climate regions, previous research was mainly conducted in the tropics and in cold climate zones [12,13,16], with very limited research in subtropical areas.
- ② Most of the research showed that SVF has a greater effect on temperature than H/W [19].
- ③ Current studies in Hong Kong are mostly focused on the effect of SVF on the urban thermal environment and rarely mention the H/W effect [22,23].

3. Research Methodology

In order to find out the influence of street canyon design factors on the urban thermal environment, several variables had to be collected. Firstly, urban geometry data were collected through field surveys and used primarily to calculate H/W. Secondly, SVF was calculated using ArcGIS-based software. Then, data measurement instruments were used to monitor the open space around the research site, and the data were compared with the Hong Kong Observatory data to verify the accuracy of the instruments. On this basis, fixed-point field measurements were made using the instruments to obtain climate data such as temperature, relative humidity, and wind speed. After obtaining the urban geometry design factor and the thermal environment evaluation index, the correlation between the independent and dependent variables was determined through regression analysis, and the dependence of the urban street canyon thermal environment on urban geometry was indicated by the coefficient of determination (R^2) value, while the range of optimal urban geometry data for the Hong Kong region in summer was derived by combining the monitored temperature with the urban geometry data obtained from the research.

3.1. Software Method for Calculating H/W

3.1.1. Calculation

In this step, the height and width of buildings on both sides of the street were measured using models of four site blocks provided by the Government of Hong Kong (HKSAR), as shown in Figure 3.

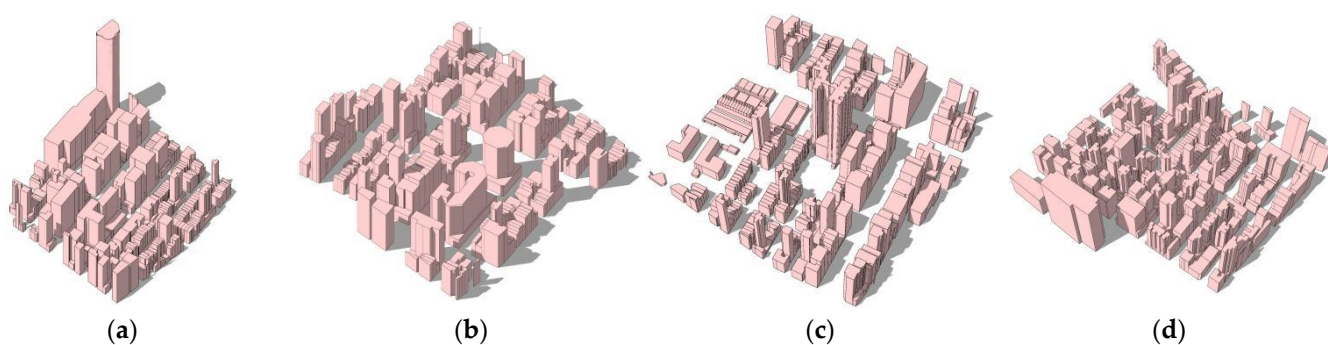


Figure 3. SketchUp models of four site blocks. (a) SketchUp models of site 1 block. (b) SketchUp models of site 2 block. (c) SketchUp models of site 3 block. (d) SketchUp models of site 4 block.

3.1.2. Validation

We visited four neighbourhoods and selected two main streets and two secondary streets in the study area: Mong Kok Road, Nathan Road, Shanghai Street, and Temple Street. The H/W data of these four streets were measured in the field and compared with the H/W values calculated from the SketchUp model data provided by the Government of Hong Kong. The results of the comparison are shown in Table 1, with an error of ≤ 0.02 . It can therefore be concluded that the H/W calculated from the urban geometry data measured by the SketchUp model is somewhat accurate and can be used as research data.

Table 1. Comparison of H/W by field measurement and SketchUp model measurement.

Measurement Method	Mong Kok Rd	Nathan Rd	Shanghai St	Temple St
H/W field measurement	0.73	2.55	1.45	1.38
SketchUp model with H/W measurement	0.72	2.54	1.45	1.39

3.2. GIS-Based Software Method for Calculating SVF

3.2.1. Calculation

In this paper, SVF is regarded as an urban geometry factor to evaluate its effect on the thermal environment. An ArcGIS-based computer program was used to calculate the SVF value of four selected urban areas, which has been proven efficient for calculating SVF in high-rise and high-density subtropical cities such as Hong Kong [8]. In this study, SVF was calculated by the SOLWEIG model [24] based on a shadow-casting algorithm and then imported into ArcGIS to generate the SVF map. The GIS-based software method uses a building database of 3D models and reconstructs the urban environment in the computer's memory, which is greatly affected by the availability of the building database. It has been widely adopted in recent studies and has the advantage of rapid calculation of continuous SVF, even for large areas [24]. Figure 4a,b show several sky views of the Mong Kok area, illustrating typical street canyons of Hong Kong with limited openness to the sky.



Figure 4. (a,b) Two sky views in typical street canyons of Mong Kok.

3.2.2. Validation

ArcGIS-based software methods that are currently used in the field of architecture have become more authoritative for computing SVF. The method was validated by Chen et al. as follows: They tested two parameterised models proposed by Oke [3] and calculated SVF by the fisheye lens photo and ArcGIS analysis methods. Then they compared the results between the two methods, which showed that the calculations by both methods were generally satisfactory. They took six photos of areas in Hong Kong with densely built buildings and scarce vegetation and used the fisheye lens calculation method and then ArcGIS to calculate SVF in the same area. The difference between the two results was small (error < 0.05), much smaller than the difference found by Gal et al. The experimental data from Chen show that GIS data analysis has good accuracy and is feasible to use in Hong Kong [3].

3.3. Field Measurement

Most of the current methods used in research on the thermal environment of outdoor streets are software simulations, but we found that simulation experiments could simplify the model, such as simplifying the scale and complexity of the neighbourhood. However, there is no fixed standard for the degree of model simplification within this discipline, and different degrees of simplification will produce different errors in the experimental results, so the resulting parameters will not fully reflect the real situation of the thermal environment. Field measurements and simulations have a sequential relationship and should be used repeatedly to verify problems after they have been identified, so field measurements are essential in this study.

3.3.1. Measurement Method

The equipment used to collect climate data for this study was a TESTO 400 (Figure 5), which measures temperature, relative humidity, and wind speed with an accuracy of ± 0.1 °C, $\pm 1.5\%$ RH, and ± 0.1 m/s, respectively. The TESTO 400 is ISO certified for use in this research. It is placed in a specified research area during the experiment, and the measurement data are used for subsequent studies.



Figure 5. TESTO 400.

3.3.2. Validation

The research team placed the TESTO 400 instrument in an open space near the measurement area to collect climate data of temperature, humidity, and wind speed for a period of 24 h on 30 October 2021 (Table 2). The average values measured by the instrument were compared with the daily averages of the Hong Kong Observatory for the day, and the difference in results were 0.3 °C for temperature, 2% for humidity, and 0.15 m/s for wind speed, which were all within the low margins of error. This demonstrated the accuracy of measurement data from this instrument.

Table 2. Statistics on measurement, weather station, and error data.

Data	Date	Measurement Period	Temperature (°C)	Humidity (%)	Wind Speed (m/s)
Hong Kong Observatory	30 October 2021	00:00–00:00 (24 h)	24.3	75	3.25
On-site measurement	30 October 2021	00:00–00:00 (24 h)	24	73	3.40
Data error	30 October 2021	00:00–00:00 (24 h)	0.3	2	0.15

3.4. Analysis Method

Regression analysis, which is a statistical process for estimating the relationship between variables, was used to predict the effects of urban street design factors on the thermal environment. The main independent variables evaluated in this paper were H/W

and SVF, and the dependent variable was air temperature. By determining the value of the correlation coefficient (R^2), the correlation between the thermal environment inside urban street canyons and the urban geometry design factors (H/W and SVF) could be determined. By comparing the magnitude of the correlation, the urban geometry design factors suitable for the study could be identified, and then the optimum factor for the summer period in the Hong Kong region could be analysed by combining the field measurement data and the actual situation. This was then combined with the field measurement data and the actual conditions in order to analyse the optimal H/W or SVF for the summer period and make recommendations for enhancing the urban outdoor environment in Hong Kong.

4. Case Study

4.1. Information Monitored in the Field

4.1.1. Basic Information of Selected Site

As Hong Kong is a densely packed city, deep street canyons are common, which means that less solar radiation will penetrate into narrow urban streets; however, they will also trap short- and long-wave radiation and reduce turbulent heat loss [25]. Four typical street canyon areas were selected as the target sites in this study to investigate the effect of urban street canyon geometry on urban thermal environment. Sites 1 and 2 are located in Mong Kok, where most buildings are commercial buildings, and sites 3 and 4 are located in Yau Ma Tei, where more buildings are residential. The general locations of the four sites are shown in Figures 6 and 7, and they show their Google Street Views of different streets at the four sites.



Figure 6. Location of four study sites.

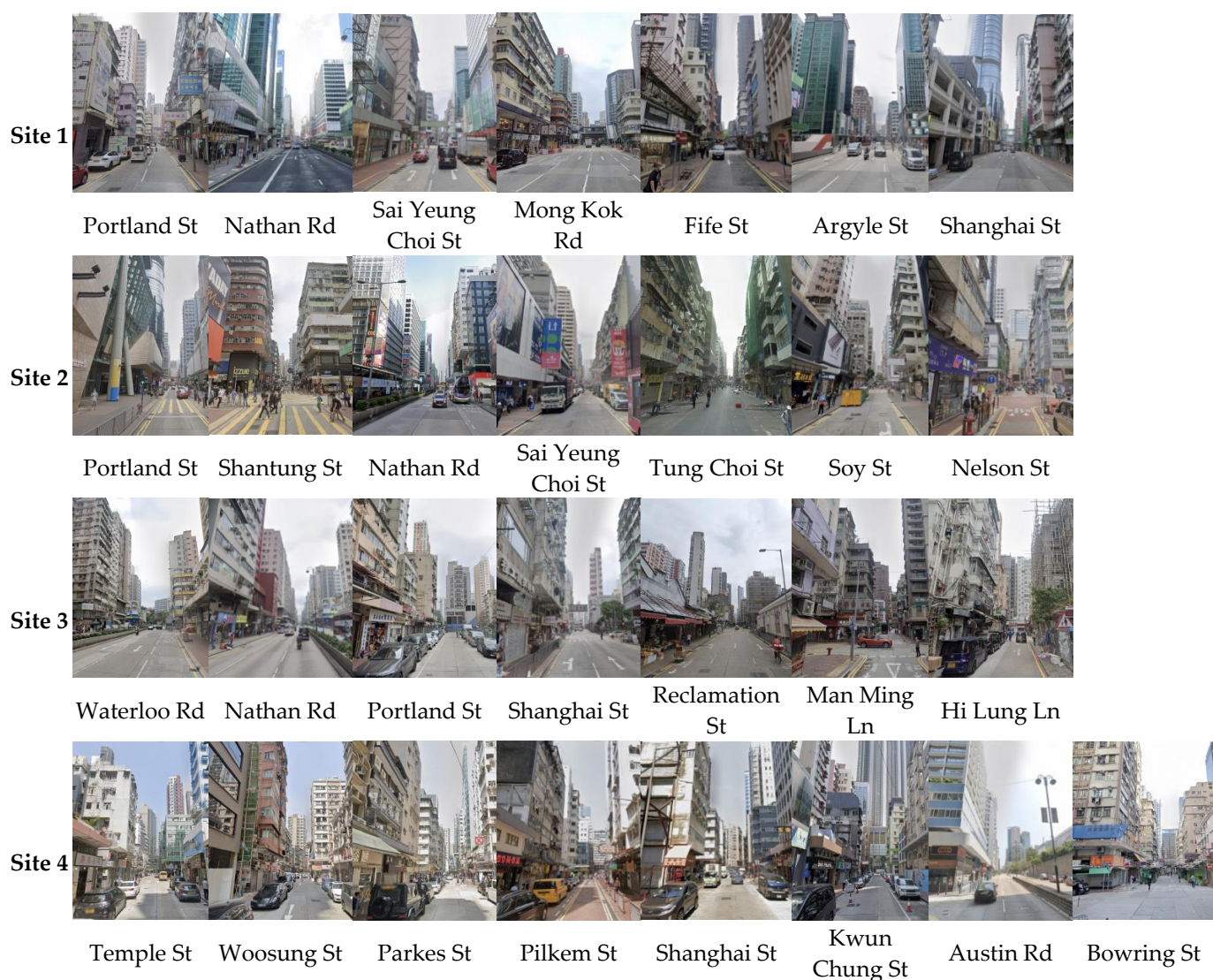


Figure 7. Realistic views of streets in different sites.

4.1.2. Measurement Time, Parameters, and Distribution of Measurement Points (MP)

The fixed field survey was carried out at four street canyons in Mong Kok and Yau Ma Tei. Four sites with a total area of $300\text{ m} \times 300\text{ m}$ were set up to cover each street in the selected area, with a total of 66 measurement points. The measurement period was 1 to 5 November 2021: site 1 on 1 November, site 2 on 2 November, site 3 on 3 November, and site 4 on 5 November. The measurement factors were temperature, humidity, and wind speed (Table 3). On-site measurement was carried out according to the different sites, with the sampling time of the data logger set at 2 s and the average measurement time for each site set at 5 min. The time interval between two adjacent measurement points was 5 min, and the average of temperature, wind speed, and humidity at each point was calculated as the reference data for this study.

Table 3. Measurement parameters.

Date	Study Site	Measurement Period	Measurement Parameters		
1 November 2021	1	13:00–15:30			
2 November 2021	2	13:00–15:25	Temperature	Humidity	Wind speed
3 November 2021	3	13:00–15:45			
5 November 2021	4	13:00–15:50			

The field measurement point distribution plan is shown in Figure 8. Each street has an average of two measurement points, one or two of which will be placed in the open space to cover the four sites. There were 16 measurement points at site 1, 15 at site 2, 17 at site 3, and 18 at site 4, for a total of 66 measurement points (Figure 8).

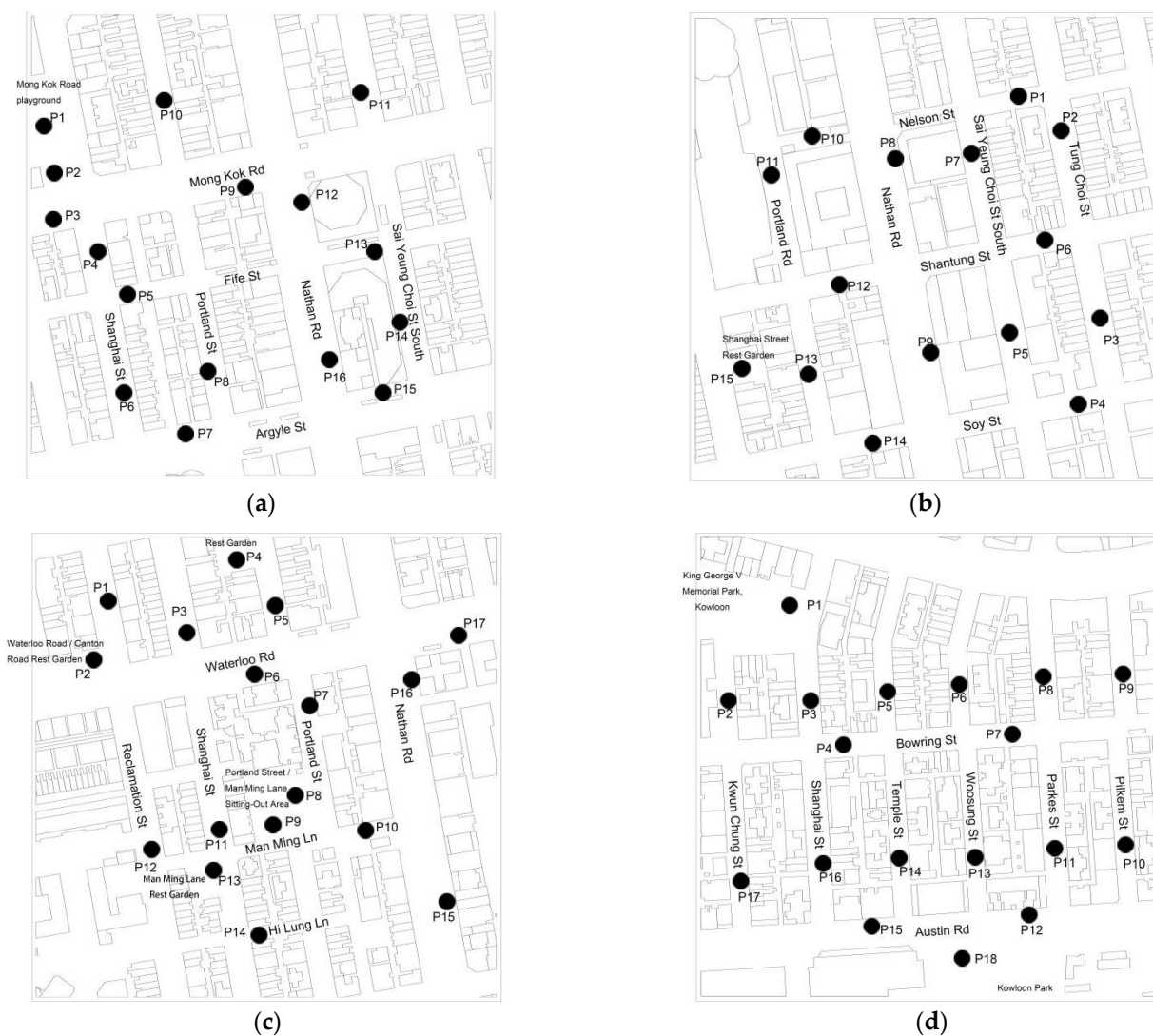


Figure 8. Plan of measurement points of different sites. (a) Plan of measurement points of site 1. (b) Plan of measurement points of site 2. (c) Plan of measurement points of site 3. (d) Plan of measurement points of site 4.

4.2. Basic Data Analysis

4.2.1. Calculation Results of H/W

The H/W of each street in the four study sites was calculated, and the values are given in Table 4. Urban street canyons in Hong Kong are usually asymmetrical, with the height of the buildings on either side of the street varying considerably depending on the location of the measurement point. The building heights were averaged over H_1 and H_2 , then H/W was analysed in this paper.

Table 4. H/W of urban streets at four study sites.

Site No.	Street Name	Points	Building Height (m)		Street Width (m)	H/W
			Left (H ₁)	Right (H ₂)		
1	Portland St	P8	41.60	23.10	15.48	2.09
		P10	43.60	55.40		3.20
	Nathan Rd	P12	45.20	70.80	30.63	1.89
		P16	48.10	69.10		1.91
	Sai Yeung Choi St South	P11	32.40	33.20	18.00	1.82
		P14	67.60	54.40		3.39
		P3	39.40	5.00		0.73
	Mong Kok Rd	P9	21.20	23.80	30.41	0.74
		P5	20.90	28.70		2.24
	Fife St	P13	16.80	67.70	11.06	3.82
		P7	57.40	53.00		1.80
	Argyle St	P15	69.10	72.10	30.60	2.31
		P4	28.70	81.40		2.79
	Shanghai St	P6	23.70	20.10	19.76	1.11
2	Portland St	P11	82.00	15.00	15.51	3.13
		P13	27.60	21.60		1.59
	Shantung St	P6	13.20	31.70	15.86	1.42
		P12	15.60	63.00		2.48
	Nathan Rd	P8	85.30	71.10	30.63	2.55
		P9	85.10	80.10		2.70
	Sai Yeung Choi St South	P5	17.60	37.00	18.39	1.48
		P7	85.30	26.60		3.04
		P2	24.30	29.90		1.48
	Tung Choi St	P3	21.70	29.40	18.26	1.40
		P4	37.10	71.00		3.26
	Soy St	P14	85.10	26.00	16.58	3.35
		P1	30.60	23.10		2.22
	Nelson St	P10	74.40	71.10	12.08	6.02
3	Waterloo Rd	P6	78.30	24.10	30.55	1.68
		P17	42.70	33.00		1.24
	Nathan Rd	P15	39.60	46.30	30.59	1.40
		P16	18.30	45.10		1.04
	Portland St	P5	30.00	53.00	15.71	2.64
		P7	120.10	25.00		4.62
	Shanghai St	P3	23.10	29.80	18.22	1.45
		P11	34.10	30.30		1.77
	Reclamation St	P1	43.70	23.40	15.94	2.10
		P12	4.00	19.40		0.73
Man Ming Ln	P10	8.10	15.70	9.19	1.29	
Hi Lung Ln	P14	22.00	20.90	9.21	2.33	
4	Temple St	P5	13.00	21.20	12.42	1.38
		P14	53.10	6.90		2.42
	Woosung St	P6	21.20	15.10	12.46	1.46
		P13	50.80	72.70		4.96
	Parkes St	P8	28.00	13.00	15.64	1.31
		P11	33.90	6.90		2.54
	Pilkem St	P9	18.80	14.10	15.92	1.03
		P10	7.00	12.20		0.60
	Shanghai St	P3	62.40	20.40	15.43	2.68
		P16	28.80	3.80		1.06
	Kwun Chung St	P2	17.10	10.10	12.55	1.08
		P17	13.10	19.80		1.31
	Austin Rd	P12	48.30	10.00	25.59	1.14
		P15	44.30	97.80		2.78
Bowring St	P4	51.60	62.10	15.80	3.60	
	P7	26.00	31.60		1.82	

Figure 9a shows the H/W at measurement points of site 1, with maximum and minimum values of 3.82 and 0.74, or a difference of 3.08. Figure 9b shows the H/W at measurement points of site 2, with maximum and minimum values of 6.02 and 1.40, or a difference of 4.62. Figure 9c shows the H/W at measurement points of site 3, with maximum and minimum values of 4.62 and 0.73, or a difference of 3.89. Figure 9d shows the H/W at measurement points of site 4, with maximum and minimum values of 4.96 and

0.60, or a difference of 4.36. The lowest variation of H/W was at site 1, and the highest was at site 2.

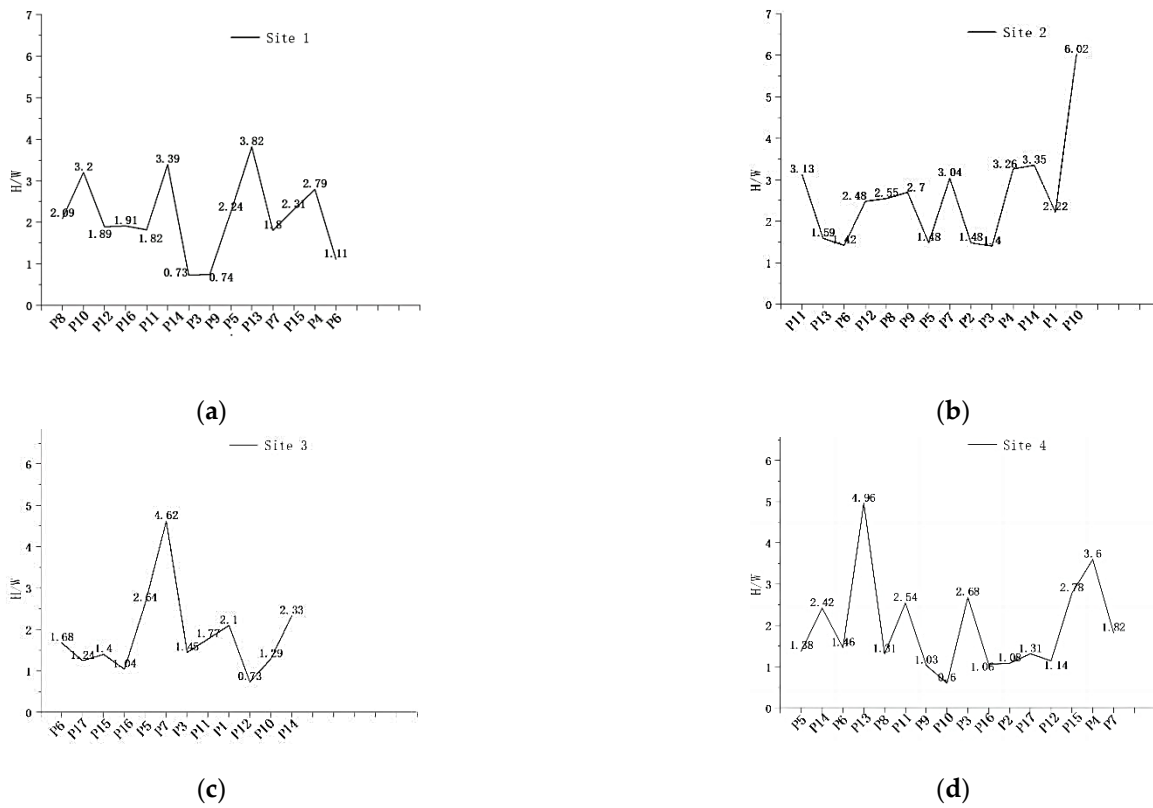


Figure 9. H/W values at measurement points of different sites. (a) H/W values at measurement points of site 1. (b) H/W values at measurement points of site 2. (c) H/W values at measurement points of site 3. (d) H/W values at measurement points of site 4.

4.2.2. Result of SVF Calculation

The SVF maps of the four study sites are shown in Figure 10. The SVF values were calculated by SOLWEIG [24] and then imported into ArcGIS.

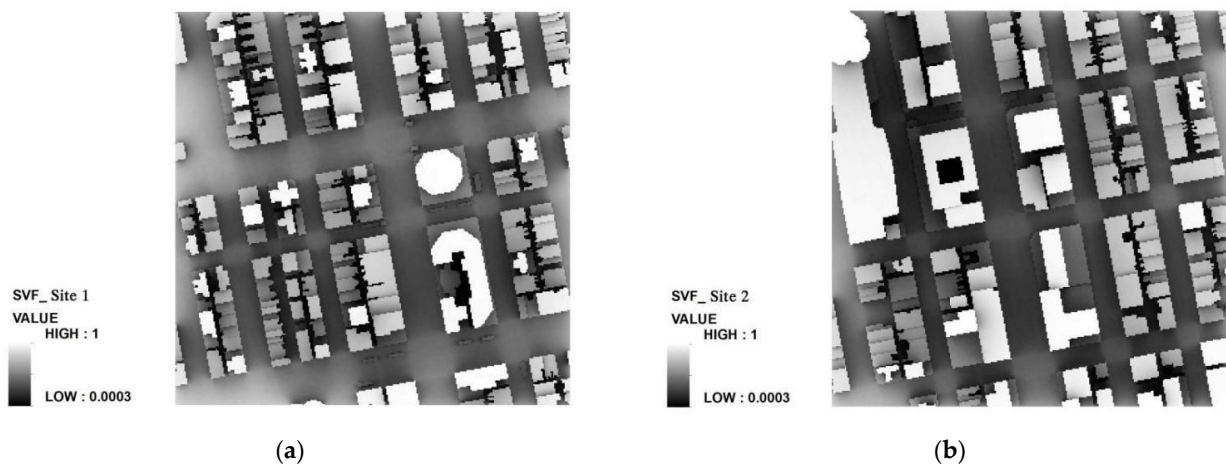


Figure 10. Cont.

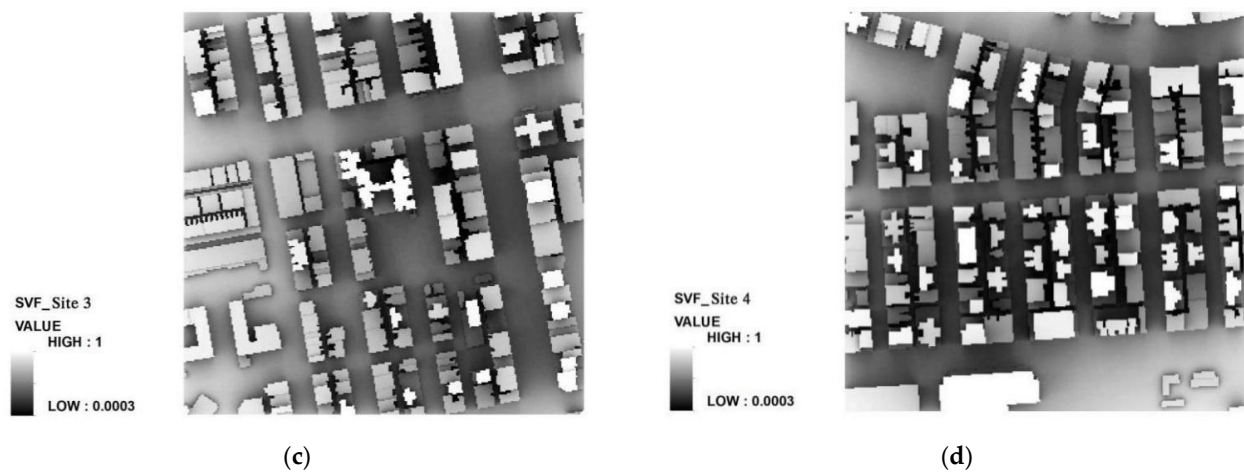


Figure 10. SVF maps of different sites. (a) SVF maps of site 1. (b) SVF maps of site 2. (c) SVF maps of site 3. (d) SVF maps of site 4.

The SVF value for each point was calculated by the average value of a $5\text{ m} \times 5\text{ m}$ rectangle with the measurement point at the centre, because the areal SVF average was proved to be more adequate to quantify the relationship between urban geometry and daytime intra-urban temperature differences than point SVF [3]. The calculated SVF values of study sites are summarised in Table 5.

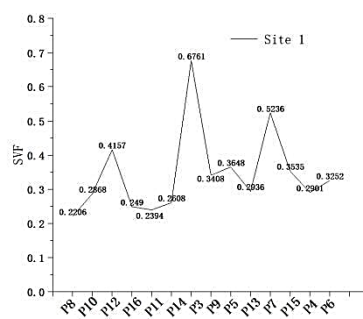
Table 5. SVF values of urban streets at four study sites.

Site No.	Urban Space	Street Name	MP	SVF
1	Street canyon	Portland St	P8	0.2206
			P10	0.2868
		Nathan Rd	P12	0.4157
			P16	0.2490
		Sai Yeung Choi St South	P11	0.2394
			P14	0.2608
		Mong Kok Rd	P3	0.6761
			P9	0.3408
		Fife St	P5	0.3648
			P13	0.2936
		Argyle St	P7	0.5236
			P15	0.3535
		Shanghai St	P4	0.2901
P6	0.3252			
2	Street canyon	Portland St	P11	0.1926
			P13	0.2092
		Shantung St	P6	0.2708
			P12	0.2201
		Nathan Rd	P8	0.2243
			P9	0.2810
		Sai Yeung Choi St South	P5	0.1989
			P7	0.1754
		Tung Choi St	P2	0.2646
			P3	0.2412
		Soy St	P4	0.2600
			P14	0.2904
		Nelson St	P1	0.1823
P10	0.0925			

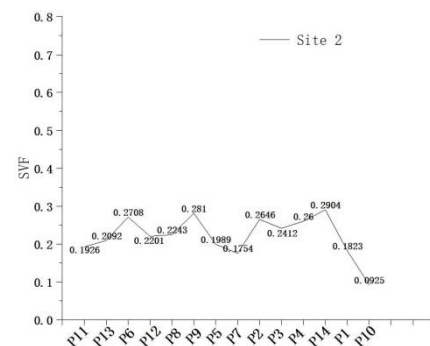
Table 5. Cont.

Site No.	Urban Space	Street Name	MP	SVF	
3	Street canyon		P6	0.3240	
			Waterloo Rd	P17	0.3424
			Nathan Rd	P15	0.3139
				P16	0.4821
			Portland St	P5	0.3926
				P7	0.2013
			Shanghai St	P3	0.3034
				P11	0.2468
			Reclamation St	P1	0.3775
			Man Ming Ln	P12	0.5913
Hi Lung Ln	P10	0.3463			
4	Street canyon		P14	0.3821	
			Temple St	P5	0.2457
			Woosung St	P14	0.1791
				P6	0.2064
			Parkes St	P13	0.1905
				P8	0.2948
			Pilkem St	P11	0.2321
				P9	0.2345
			Shanghai St	P10	0.2441
				P3	0.2590
			Kwun Chung St	P16	0.1881
				P2	0.3764
			Austin Rd	P17	0.2699
			Bowring St	P12	0.5619
P15	0.2321				
	P4	0.3175			
	P7	0.2777			

Figure 11a shows SVF at measurement points of site 1, with maximum and minimum values of 0.6761 and 0.2206, or a difference of 0.4555. Figure 11b shows SVF at measurement points of site 2, with maximum and minimum values of 0.2904 and 0.0925, or a difference of 0.1979. Figure 11c shows SVF at measurement points of site 3, with maximum and minimum values of 0.5913 and 0.2013, or a difference of 0.3900. Figure 11d shows SVF at measurement points of site 4, with maximum and minimum values of 0.5619 and 0.1791, or a difference of 0.3828. The smallest change in SVF was at site 2, and the largest was at site 1.



(a)



(b)

Figure 11. Cont.

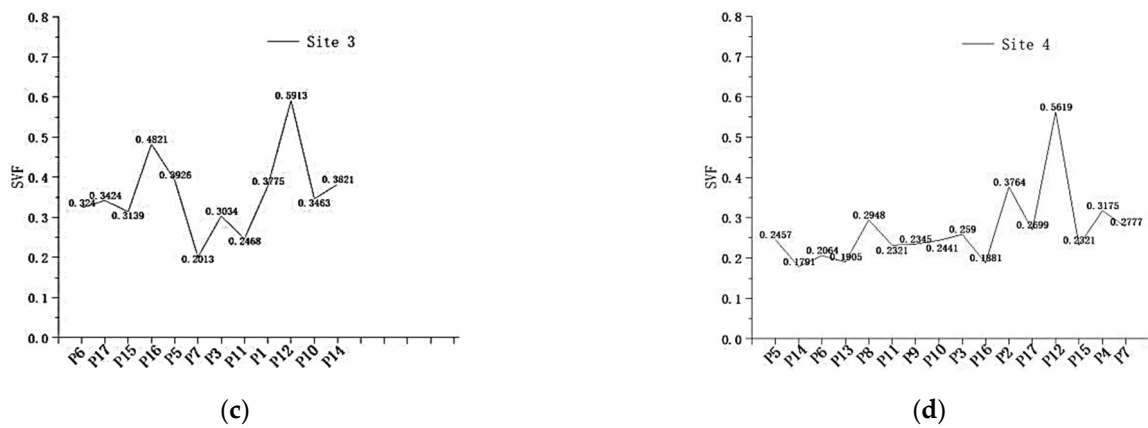


Figure 11. SVF at measurement points of different sites. (a) SVF at measurement points of site 1. (b) SVF at measurement points of site 2. (c) SVF at measurement points of site 3. (d) SVF at measurement points of site 4.

4.2.3. Result of Field Measurement

Table 3 lists urban climate data, including temperature (T), relative humidity (RH), and wind speed (V), corresponding to the measurement points of every street at the four study sites, along with average values for these parameters.

By collating field measurement data from Table 4, we categorised humidity, temperature, and wind speed into four levels, A, B, C, and D, with temperature ranges of 30–31 °C, 29–30 °C, 28–29 °C, and 27–28 °C; humidity of 72–78%, 66–72%, 60–66%, 54–60%; and wind speed of 1.2–1.6 m/s, 0.8–1.2 m/s, 0.4–0.8 m/s, and 0–0.4 m/s, respectively. Combined with the field measurements, the spatial distribution of temperature, humidity, and wind speed in each urban street canyon is shown in the figures as follows.

The temperature distribution of measurement points at site 1 is shown in Figure 12a. There are seven measurement points at temperature level C and six at level D. Figure 12b shows the temperature distribution of measurement points at site 2, with eleven measurement points at temperature level C and three points at level D. Figure 12c shows that there are eight measurement points at level C and a few at level B and level D. The temperature distribution of measurement points at site 4 shows eleven at level B and three at level C in Figure 12d. Overall, the distribution of temperature level at site 4 is dominated by A, B, and C, with the highest average temperature, while site 2 is dominated by C, with the lowest average temperature.

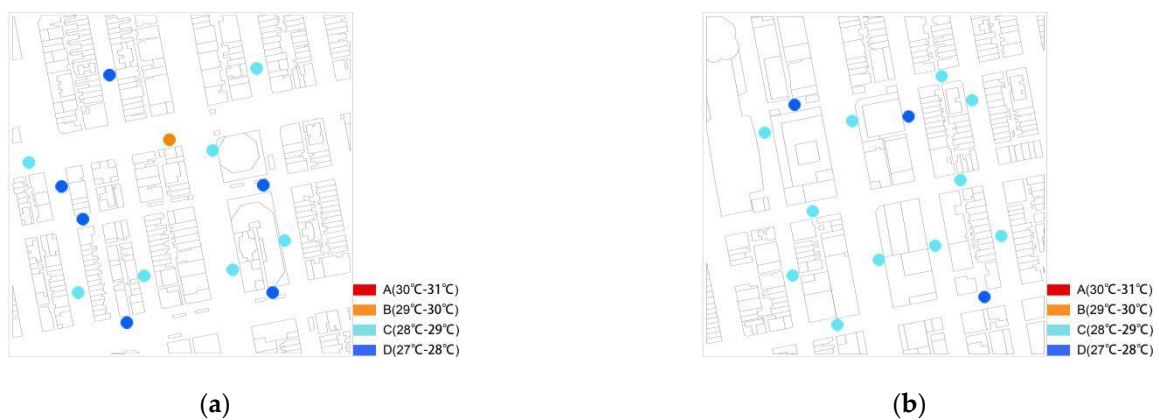


Figure 12. Cont.



Figure 12. Temperature distribution of measurement points at different sites. (a) Temperature distribution of measurement points at site 1 on 1 November 2021. (b) Temperature distribution of measurement points at site 2 on 2 November 2021. (c) Temperature distribution of measurement points at site 3 on 3 November 2021. (d) Temperature distribution of measurement points at site 4 on 5 November 2021.

Figure 13a shows that wind speed at site 1 is mainly at level B, distributed over eight measurement points. Figure 13b shows that there are five measurement points at site 2 with level B wind speed and five at level C. There are two points at site 3 with level A wind speed, five with level B, and five with level C (Figure 13c). There is a maximum of ten measurement points with level C wind speed and three with level B at site 4 (Figure 13d).

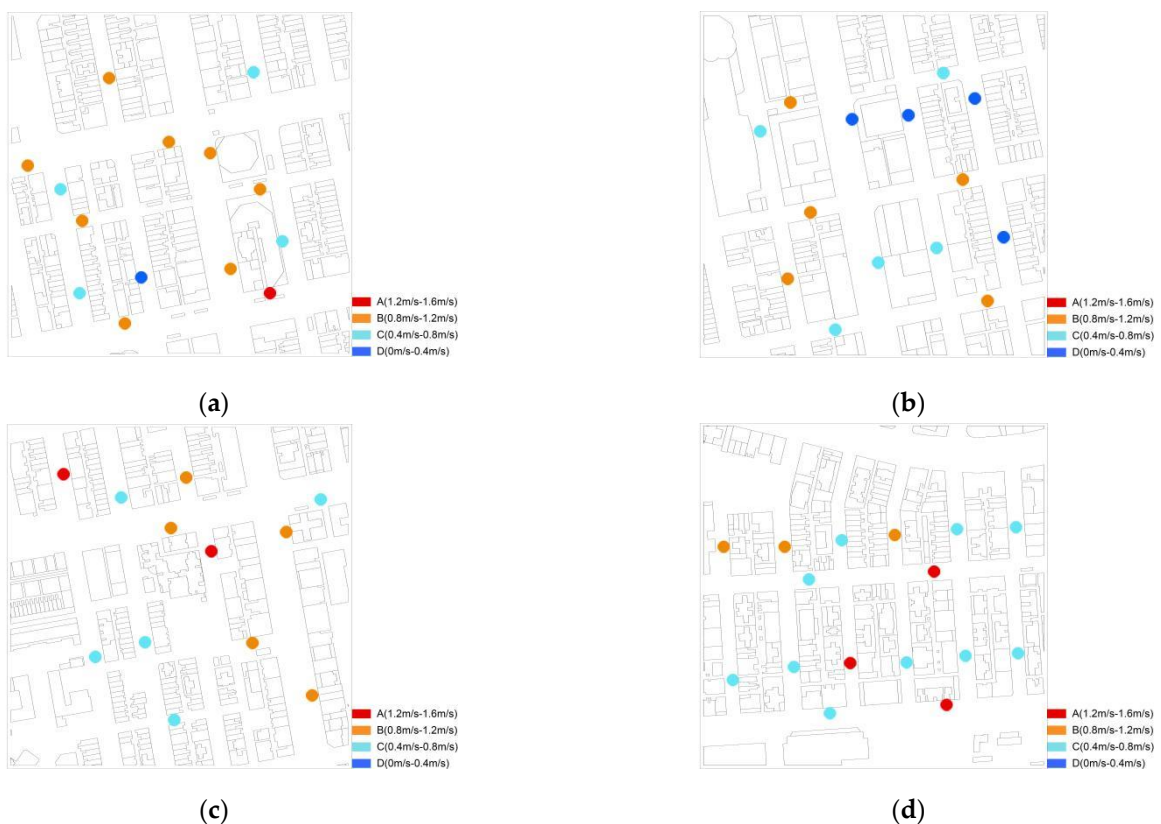


Figure 13. Wind speed distribution of measurement points at different sites. (a) Wind speed distribution of measurement points at site 1 on 1 November 2021. (b) Wind speed distribution of measurement points at site 2 on 2 November 2021. (c) Wind speed distribution of measurement points at site 3 on 3 November 2021. (d) Wind speed distribution of measurement points at site 4 on 5 November 2021.

As can be seen in Figure 14, there are eight measurement points at site 1 with level B humidity, five with level C, and only one with level D (Figure 14a). Figure 14b shows that there is one measurement point at site 2 with level A humidity, eleven with level B, and two with level C. The distribution at site 3 shows that there are five measurement points with level A humidity and seven with level B (Figure 14c). Figure 14d shows that there are ten measurement points with level C humidity and six with level D at site 4. It can be seen that the overall humidity is higher at site three and lower at site 4.

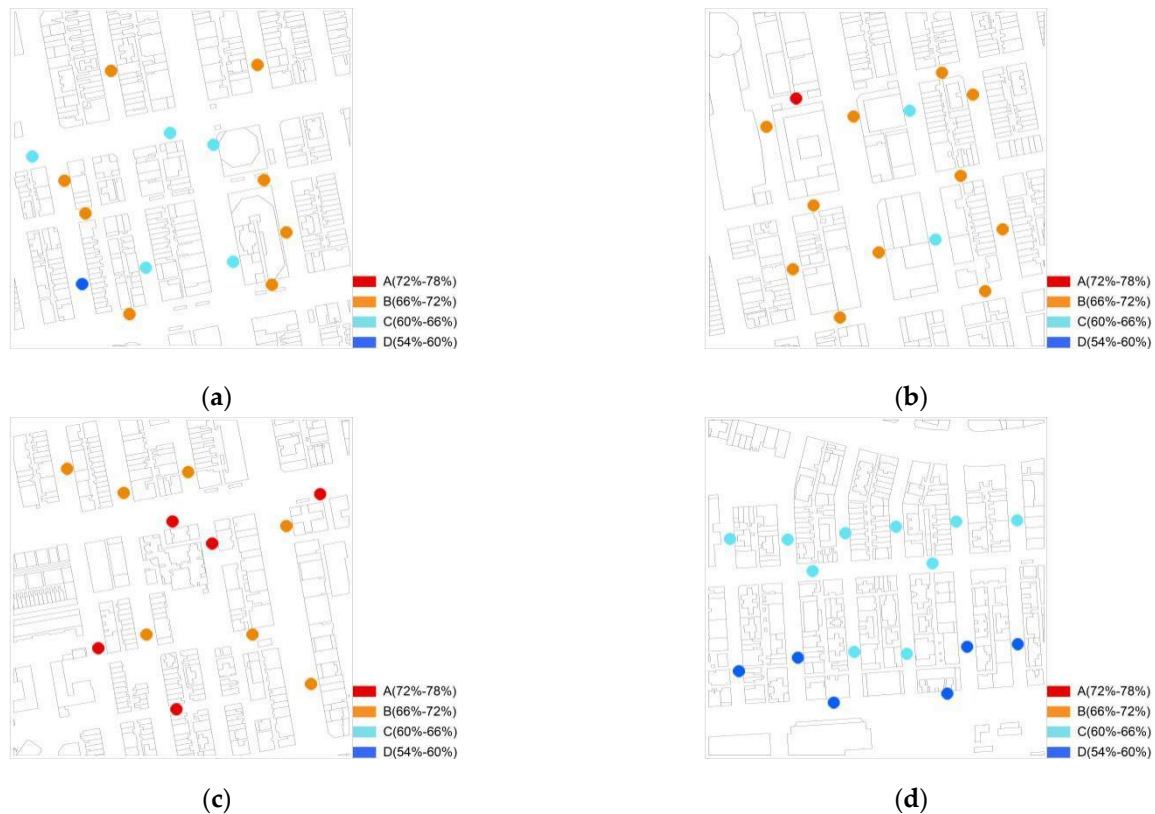


Figure 14. Humidity distribution of measurement points in different sites. (a) Humidity distribution of measurement points in site 1 on 1 November 2021. (b) Humidity distribution of measurement points in site 2 on 2 November 2021. (c) Humidity distribution of measurement points in site 3 on 3 November 2021. (d) Humidity distribution of measurement points in site 4 on 5 November 2021.

4.3. Regression Analysis

Table 6 provides a reliable record of the outdoor temperature, wind speed, humidity and the H/W and SVF values at each measurement point, which is used as a data resource for the subsequent calculation of the correlation between H/W and SVF values and temperature respectively, and for comparing the correlation in this study.

Table 6. Summary of thermal environmental parameter and SVF and H/W.

Site NO.	Urban Space	Name	MP	H/W	SVF	Ta (°C)	RH (%)	V (m/s)
1	Street canyon	Portland St	P8	2.09	0.2206	28.44	64.30	0.22
			P10	3.20	0.2868	27.82	66.59	0.81
		Nathan Rd	P12	1.89	0.4157	28.89	64.01	1.03
			P16	1.91	0.2490	28.83	63.73	0.85
		Sai Yeung Choi St South	P11	1.82	0.2394	28.24	67.64	0.58
			P14	3.39	0.2608	28.02	66.53	0.67
		Mong Kok Rd	P3	0.73	0.6761	28.87	65.64	0.85
			P9	0.74	0.3408	29.07	63.91	1.00
		Fife St	P5	2.24	0.3648	27.98	66.66	0.96
		Argyle St	P13	3.82	0.2936	27.80	68.07	0.98
			P7	1.80	0.5236	27.99	67.75	0.94
		Shanghai St	P15	2.31	0.3535	27.38	69.41	1.20
P4	2.79		0.2901	27.79	66.73	0.71		
			P6	1.11	0.3252	28.70	65.02	0.59
2	Street canyon	Portland St	P11	3.13	0.1926	28.13	71.44	0.54
			P13	1.59	0.2092	28.54	68.40	0.99
		Shantung St	P6	1.42	0.2708	28.38	68.15	1.01
			P12	2.48	0.2201	28.36	70.61	1.07
		Nathan Rd	P8	2.55	0.2243	28.74	67.51	0.83
			P9	2.70	0.2810	28.93	69.14	0.61
		Sai Yeung Choi St South	P5	1.48	0.1989	28.54	65.53	0.41
			P7	3.04	0.1754	27.80	65.22	0.38
		Tung Choi St	P2	1.48	0.2646	28.46	69.62	0.35
			P3	1.40	0.2412	28.57	69.03	0.31
		Soy St	P4	3.26	0.2600	27.51	69.79	0.99
			P14	3.35	0.2904	28.07	71.58	0.77
Nelson St	P1	2.22	0.1823	28.39	68.18	0.64		
	P10	6.02	0.0925	27.40	72.15	0.85		
3	Street canyon	Waterloo Rd	P6	1.68	0.3240	28.14	73.43	1.06
			P17	1.24	0.3424	28.65	72.33	0.78
		Nathan Rd	P15	1.40	0.3139	28.88	70.81	0.82
			P16	1.04	0.4821	29.00	70.80	0.91
		Portland St	P5	2.64	0.3926	28.46	71.69	0.94
			P7	4.62	0.2013	27.45	75.87	1.56
		Shanghai St	P3	1.45	0.3034	28.41	70.91	0.74
			P11	1.77	0.2468	28.28	71.92	0.43
		Reclamation St	P1	2.10	0.3775	27.92	71.65	1.56
			P12	0.73	0.5913	28.40	72.06	0.74
		Man Ming Ln	P10	1.29	0.3463	29.26	71.31	0.97
		Hi Lung Ln	P14	2.33	0.3821	28.07	74.30	0.43
4	Street canyon	Temple St	P5	1.38	0.2457	29.42	61.81	0.72
			P14	2.42	0.1791	28.49	61.24	1.45
		Woosung St	P6	1.46	0.2064	29.14	62.96	1.02
			P13	4.96	0.1905	27.75	63.54	0.75
		Parkes St	P8	1.31	0.2948	29.23	61.80	0.49
			P11	2.54	0.2321	30.14	59.68	0.65
		Pilkem St	P9	1.03	0.2345	29.47	60.01	0.75
			P10	0.60	0.2441	29.95	58.61	0.72
		Shanghai St	P3	2.68	0.2590	28.51	64.76	1.13
			P16	1.06	0.1881	29.60	55.02	0.72
		Kwun Chung St	P2	1.08	0.3764	29.35	62.48	0.97
			P17	1.31	0.2699	29.47	56.40	0.40
Austin Rd	P12	1.14	0.5619	29.73	58.71	1.22		
	P15	2.78	0.2321	29.55	57.80	0.67		
Bowring St	P4	3.60	0.3175	28.76	64.45	0.51		
	P7	1.82	0.2777	29.22	64.50	1.26		

4.3.1. Regression between H/W and Temperature

The relationship between air temperature and H/W of the four study sites is shown separately in Figure 15 based on the different climate conditions of the four field measurement periods. Through regression analysis of measurement point data, the linear correlation of air temperature and H/W for each site was generated. All four study sites show that H/W has a negative effect on air temperature (2 m above ground level) within street canyons, with the coefficient of determination (R^2) ranging from 0.5232 to 0.5463 (Table 7). Site 2 shows the highest correlation, and site 4 has the relatively lowest correlation between air temperature and H/W. In general, H/W is an efficient parameter to use in evaluating the effect of shading of urban street canyons on the thermal environment.

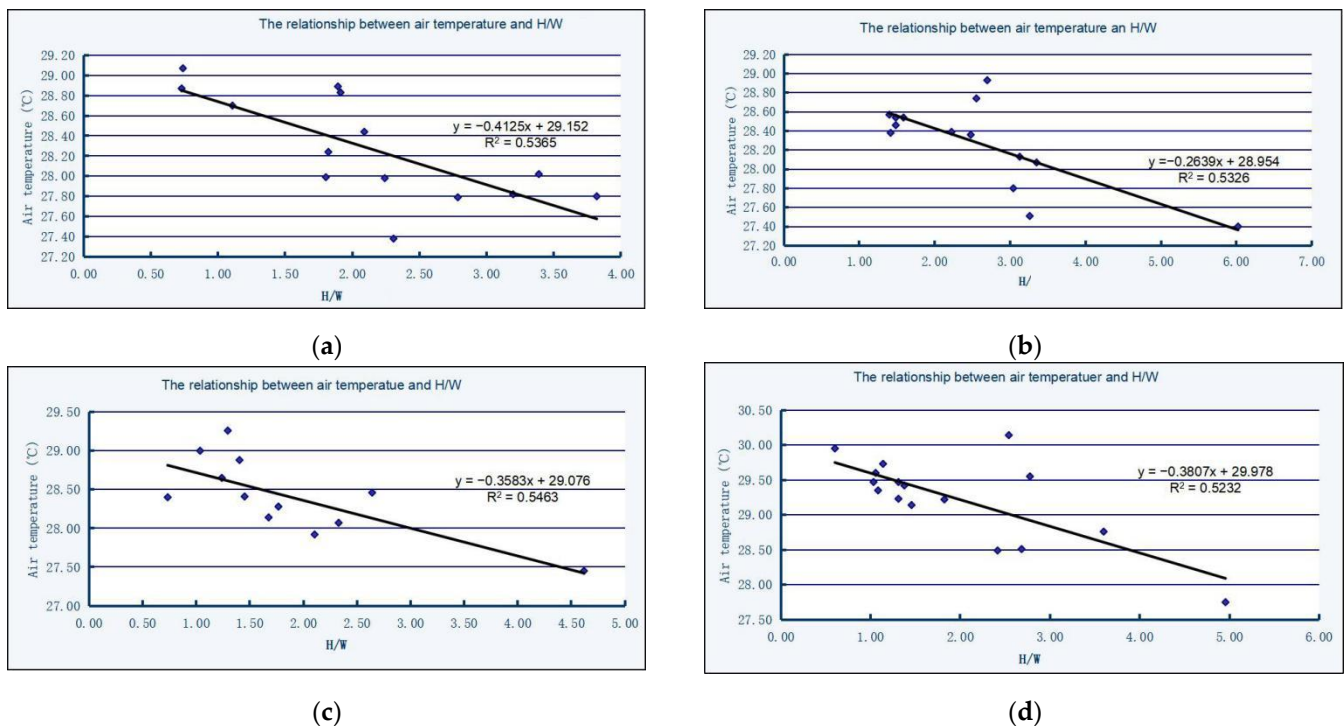


Figure 15. Relationship between air temperature (2 m above ground) and H/W of different sites. (a) Relationship between air temperature (2 m above ground) and H/W of site 1. (b) Relationship between air temperature (2 m above ground) and H/W of site 2. (c) Relationship between air temperature (2 m above ground) and H/W of site 3. (d) Relationship between air temperature (2 m above ground) and H/W of site 4.

Table 7. Summary of H/W and temperature correlation at each site.

Site No.	Regression Equation	R^2	α (%)
1	$\Delta T = -0.4125 \times H/W + 29.152$	0.5365	5
2	$\Delta T = -0.2639 \times H/W + 28.954$	0.5326	5
3	$\Delta T = -0.3583 \times H/W + 29.076$	0.5463	5
4	$\Delta T = -0.3807 \times H/W + 29.978$	0.5232	5

4.3.2. Regression between SVF and Temperature

The relationship between air temperature and SVF of the four study sites is shown separately in Figure 16. Through regression analysis of measurement point data, the linear correlation of air temperature and SVF for each site was generated. Regression equations of all four sites show a slightly positive effect of SVF on air temperature, which means that air temperature increases with increased SVF (Figure 16). However, the correlation of SVF and air temperature is quite low, with the relatively highest determination coefficient (R^2) of

0.2120 for site 2 and the relatively lowest R^2 of 0.0523 for site 1 (Table 8). Compared with the correlation of air temperature and H/W, SVF has a relatively weaker effect on temperature.

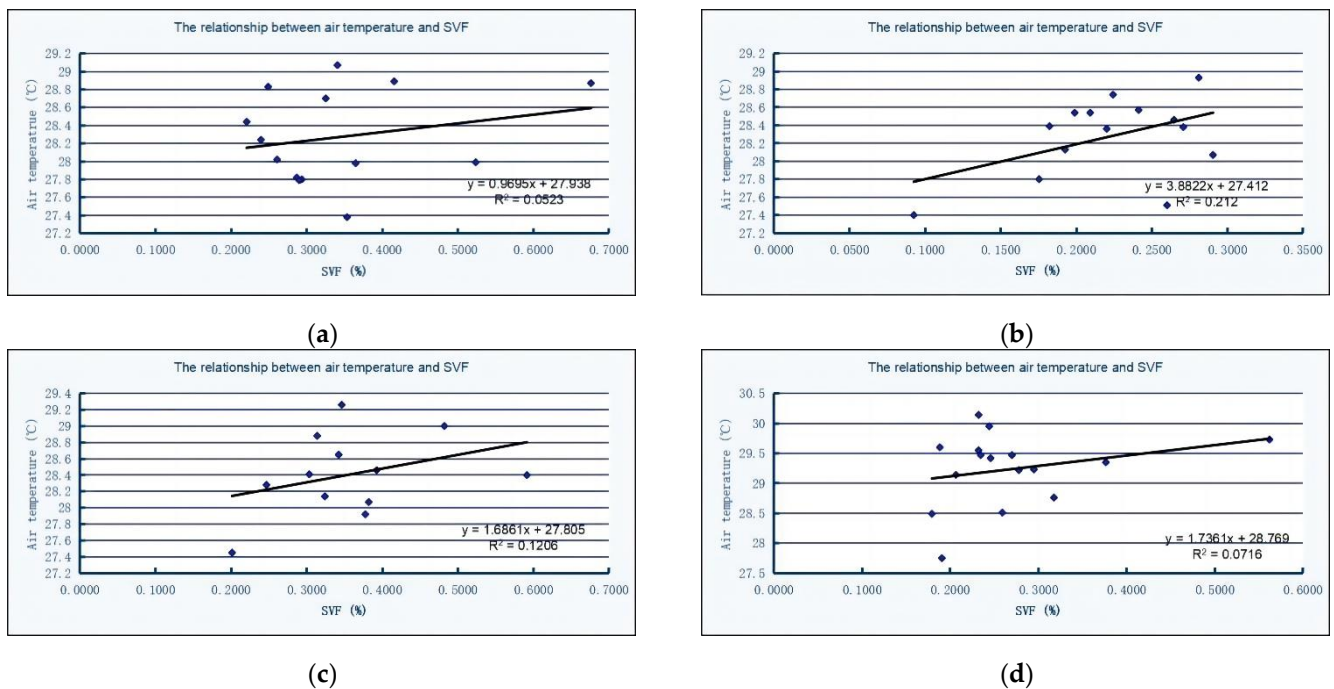


Figure 16. Relationship between air temperature (2 m above ground) and SVF at different sites. (a) Relationship between air temperature (2 m above ground) and SVF at site 1. (b) Relationship between air temperature (2 m above ground) and SVF at site 2. (c) Relationship between air temperature (2 m above ground) and SVF at site 3. (d) Relationship between air temperature (2 m above ground) and SVF at site 4.

Table 8. Summary of SVF and temperature correlation at each measurement point.

Site No.	Regression Equation	R^2	α (%)
1	$\Delta T = 0.9695 \times \text{SVF} + 27.938$	0.0523	5
2	$\Delta T = 3.8822 \times \text{SVF} + 27.412$	0.2120	5
3	$\Delta T = 1.6861 \times \text{SVF} + 27.805$	0.1206	5
4	$\Delta T = 1.7361 \times \text{SVF} + 28.769$	0.0716	5

By combining the graph of the relationship between point measurement temperature and H/W (Figure 17), it can be seen that outdoor temperature and H/W are not exactly linearly correlated. When H/W = 2.31, the outdoor temperature reaches a minimum of 27.38 °C, and when H/W = 2.54, the outdoor temperature reaches a maximum of 30.14 °C.

The research period was the summer season in Hong Kong. Due to the high population density and high summer temperature in Hong Kong, it is appropriate to reduce the outdoor temperature. Combining the analyses, H/W of 2.09–2.48 and H/W > 3.6 are the most suitable values for Hong Kong in summer (Figure 17).

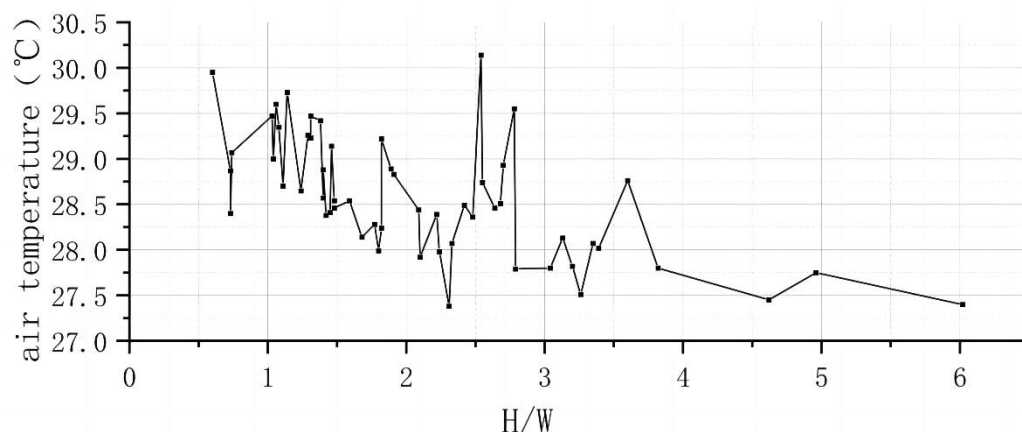


Figure 17. Summary of SVF and temperature correlation at each site.

5. Conclusions and Further Study

This paper investigates the relevance of the urban street canyon thermal environment to urban geometry factors and the extent to which different urban geometry factors affect the microclimate of urban streets in a subtropical, high-density city, Hong Kong. Field measurements were conducted in early November 2021 to obtain climate data, including temperature, wind speed, and relative humidity, for urban street canyons located in Mong Kok and Yau Ma Tei. Through a review of the literature, it was obtained that H/W and SVF are the main factors influencing urban street geometry, leading to the following conclusions.

5.1. Conclusions

- ① The regression analysis showed a negative correlation between H/W and daytime air temperature at the four sites, with a mean coefficient of determination (R^2) of 0.5347. SVF can also be used to indicate the level of shading within street canyons, which showed a positive correlation with air temperature during the measurement period. However, the correlation between SVF and air temperature is low, with a mean R^2 of 0.1141, which is much lower than the correlation between H/W and air temperature. In summary, H/W has a greater effect on the thermal environment than SVF, which also suggests that H/W is a more effective parameter for urban planners to use in improving the thermal environment within urban street canyons and thermal comfort at the pedestrian level.
- ② The field research sites are located in typical high-density neighbourhoods in Hong Kong; combining H/W obtained from the field survey, it can be seen that H/W varies greatly between areas due to differences in functional organisation and road levels; the lowest H/W was 0.60, and the highest was 6.02, giving a variance of 5.42. Further analysis of the data showed that H/W in this typical area lies between 0.60 and 6.02, with an average of 2.13.
- ③ Combining the graph of the relationship between point measurement temperature and H/W, it can be seen that outdoor temperature and H/W are not exactly linearly correlated, with the outdoor temperature reaching a minimum of 27.38 °C with H/W of 2.31 and a maximum of 30.14 °C with H/W of 2.54. Combining the analysis of the graphs, it can be seen that outdoor temperature is lower with H/W values of 2.31–2.48 and 3.35–3.60, and the temperature rises as H/W increases. The reason for this phenomenon is presumably because, within this range, H/W is the dominant factor affecting the outdoor air temperature in the city, so the temperature rises at the same time H/W increases. When H/W is 2.09–2.31 and H/W > 3.60, the outdoor air temperature is low and tends to decrease. It is assumed that within this H/W range, building shading is the dominant factor, and as building heights rise, solar radiation received by the street decreases throughout the day due to the mutual shading of buildings, and the temperature tends to decrease gradually.

5.2. Further Research

Our further research should focus on studying a single variable factor of the effect of street H/W on the thermal environment under typical summer conditions in Hong Kong. Field measurements should be carried out during the hot summer months, and climate data should be collected from each measurement point simultaneously as much as possible to control for variables. In addition, different weather conditions, such as sunny and cloudy, can also have an effect on temperature, which also needs to be considered. In addition to urban geometry, other factors such as greenery, building materials, road albedo, and anthropogenic heat can have different effects on the thermal environment, which also need to be studied and analysed in further work.

Author Contributions: Conceptualization and methodology, S.Z. and X.M.; investigation, S.Z., M.C. and S.L.; data curation and writing—review and editing, M.C. and S.L.; software, S.Z. and S.L.; supervision, X.M. All authors have read and agreed to the published version of the manuscript.

Funding: This research was funded by the Sichuan Provincial Youth Scientific and Technological Innovation Research Team on Ecological Adaptability of Plateau Architecture, grant number 2022JDTD0008.

Institutional Review Board Statement: Not applicable.

Informed Consent Statement: Not applicable.

Data Availability Statement: Not applicable.

Conflicts of Interest: The authors declare no conflict of interest.

References

1. Climate of Hong Kong. Available online: <https://www.hko.gov.hk/en/cis/climahk.htm> (accessed on 12 October 2022).
2. Hong Kong Population 2022 (Demographics, Maps, Graphs). Available online: <https://worldpopulationreview.com/countries/hong-kong-population> (accessed on 12 October 2022).
3. Chen, L.; Ng, E.; An, X.; Ren, C.; Lee, M.; Wang, U.; He, Z. Sky View Factor Analysis of Street Canyons and Its Implications for Daytime Intra-Urban Air Temperature Differentials in High-Rise, High-Density Urban Areas of Hong Kong: A GIS-Based Simulation Approach: GIS-BASED SVF ANALYSIS AND APPLICATION IN HONG KONG. *Int. J. Climatol.* **2012**, *32*, 121–136. [[CrossRef](#)]
4. World's Greatest Urban Hike—Hong Kong Island. Available online: <https://asiabooksandtravel.com/greatest-urban-hike-hong-kong/> (accessed on 12 October 2022).
5. Hong Kong Considers Reopening Borders with 11 Countries. Available online: <https://www.traveloffpath.com/hong-kong-considering-reopening-borders-with-11-countries/> (accessed on 12 October 2022).
6. Gong, F.-Y.; Zeng, Z.-C.; Zhang, F.; Li, X.; Ng, E.; Norford, L.K. Mapping Sky, Tree, and Building View Factors of Street Canyons in a High-Density Urban Environment. *Build. Environ.* **2018**, *134*, 155–167. [[CrossRef](#)]
7. Chatzipoulka, C.; Compagnon, R.; Nikolopoulou, M. Urban Geometry and Solar Availability on Façades and Ground of Real Urban Forms: Using London as a Case Study. *Sol. Energy* **2016**, *138*, 53–66. [[CrossRef](#)]
8. Han, D.; Zhang, T.; Qin, Y.; Tan, Y.; Liu, J. A Comparative Review on the Mitigation Strategies of Urban Heat Island (UHI): A Pathway for Sustainable Urban Development. *Clim. Dev.* **2022**, 1–25. [[CrossRef](#)]
9. Gong, F.-Y.; Zeng, Z.-C.; Ng, E.; Norford, L.K. Spatiotemporal Patterns of Street-Level Solar Radiation Estimated Using Google Street View in a High-Density Urban Environment. *Build. Environ.* **2019**, *148*, 547–566. [[CrossRef](#)]
10. Ali-Toudert, F.; Mayer, H. Thermal Comfort in an East–West Oriented Street Canyon in Freiburg (Germany) under Hot Summer Conditions. *Theor. Appl. Climatol.* **2007**, *87*, 223–237. [[CrossRef](#)]
11. Emmanuel, R.; Johansson, E. Influence of Urban Morphology and Sea Breeze on Hot Humid Microclimate: The Case of Colombo, Sri Lanka. *Clim. Res. Clim. RES* **2006**, *30*, 189–200. [[CrossRef](#)]
12. Johansson, E. Influence of Urban Geometry on Outdoor Thermal Comfort in a Hot Dry Climate: A Study in Fez, Morocco. *Build. Environ.* **2006**, *41*, 1326–1338. [[CrossRef](#)]
13. Acero, J.A.; Koh, E.J.Y.; Ruefenacht, L.A.; Norford, L.K. Modelling the Influence of High-Rise Urban Geometry on Outdoor Thermal Comfort in Singapore. *Urban Clim.* **2021**, *36*, 100775. [[CrossRef](#)]
14. Muniz-Gaal, L.P.; Pezzuto, C.C.; de Carvalho, M.F.H.; Mota, L.T.M. Urban Geometry and the Microclimate of Street Canyons in Tropical Climate. *Build. Environ.* **2020**, *169*, 106547. [[CrossRef](#)]
15. Muniz-Gaal, L.P.; Pezzuto, C.C.; de Carvalho, M.F.H.; Mota, L.T.M. Urban Legislation and Thermal Comfort in Urban Street Canyons: A Case Study in Campinas. *Ambiente Construído* **2018**, *18*, 177–196. [[CrossRef](#)]

16. Sun, C.; Lian, W.; Liu, L.; Dong, Q.; Han, Y. The Impact of Street Geometry on Outdoor Thermal Comfort within Three Different Urban Forms in Severe Cold Region of China. *Build. Environ.* **2022**, *222*, 109342. [[CrossRef](#)]
17. Oke, T.R. Canyon Geometry and the Nocturnal Urban Heat Island: Comparison of Scale Model and Field Observations. *J. Climatol.* **1981**, *1*, 237–254. [[CrossRef](#)]
18. Krüger, E.L.; Minella, F.O.; Rasia, F. Impact of Urban Geometry on Outdoor Thermal Comfort and Air Quality from Field Measurements in Curitiba, Brazil. *Build. Environ.* **2011**, *46*, 621–634. [[CrossRef](#)]
19. He, X.; Miao, S.; Shen, S.; Li, J.; Zhang, B.; Zhang, Z.; Chen, X. Influence of Sky View Factor on Outdoor Thermal Environment and Physiological Equivalent Temperature. *Int. J. Biometeorol.* **2015**, *59*, 285–297. [[CrossRef](#)]
20. Ibrahim, A.A.; Nduka, I.; Iguisi, E.O.; Ati, O. An Assessment of the Impact of Sky View Factor (SVF) on the Micro-Climates of Urban Kano. *Aust. J. Basic Appl. Sci.* **2011**, *5*, 81–85.
21. Bourbia, F.; Boucheriba, F. Impact of Street Design on Urban Microclimate for Semi Arid Climate (Constantine). *Renew. Energy* **2010**, *35*, 343–347. [[CrossRef](#)]
22. Deevi, B.; Chundeli, F.A. Quantitative Outdoor Thermal Comfort Assessment of Street: A Case in a Warm and Humid Climate of India. *Urban Clim.* **2020**, *34*, 100718. [[CrossRef](#)]
23. Xiong, K.; Yang, Z.; Cheng, C. Microclimate Environmental Assessment and Impact of Mountain City Pedestrian Streets in Summer. *E3S Web Conf.* **2020**, *172*, 11001. [[CrossRef](#)]
24. Lindberg, F.; Holmer, B.; Thorsson, S. SOLWEIG 1.0—Modelling Spatial Variations of 3D Radiant Fluxes and Mean Radiant Temperature in Complex Urban Settings. *Int. J. Biometeorol.* **2008**, *52*, 697–713. [[CrossRef](#)]
25. Pearlmutter, D.; Berliner, P.; Shaviv, E. Integrated Modeling of Pedestrian Energy Exchange and Thermal Comfort in Urban Street Canyons. *Build. Environ.* **2007**, *42*, 2396–2409. [[CrossRef](#)]